Available online at www.sciencedirect.com
ScienceDirect
Mathematical Biosciences 207 (2007) 352–364
Mathematical Biosciences
www.elsevier.com/locate/mbs

Scaling properties of pyramidal neurons in mice neocortex

Andreas Schierwagen [a,*], Alán Alpár [b], Ulrich Gärtner [b]

[a] *Institute for Computer Science, University of Leipzig, 04109 Leipzig, Germany*
[b] *Department of Neuroanatomy, Paul Flechsig Institut for Brain Research, University of Leipzig, 04109 Leipzig, Germany*

Received 2 June 2006; received in revised form 21 August 2006; accepted 24 August 2006
Available online 5 September 2006

Abstract

Dendritic morphology is the structural correlate for receiving and processing inputs to a neuron. An interesting question then is what the design principles and the functional consequences of enlarged or shrinked dendritic trees might be. As yet, only a few studies have examined the effects of neuron size changes. Two theoretical scaling modes have been analyzed, conservative (isoelectrotonic) scaling (preserves the passive and active response properties) and isometric scaling (steps up low pass-filtering of inputs). It has been suggested that both scaling modes were verified in neuroanatomical studies. To overcome obvious limitations of these studies like small size of analyzed samples and restricted validity of utilized scaling measures, we considered the scaling problem of neurons on the basis of large sample data and by employing a more general method of scaling analysis. This method consists in computing the morphoelectrotonic transform (MET) of neurons. The MET maps the neuron from anatomical space into electrotonic space using the logarithm of voltage attenuation as the distance metric. The theory underlying this approach is described and then applied to two samples of morphologically reconstructed pyramidal neurons (cells from neocortex of wildtype and synRas transgenic mice) using the NEURON simulator. In a previous study, we could verify a striking increase of dendritic tree size in synRas pyramidal neurons. Surprisingly, in this study the statistical analysis of the sample MET dendrograms revealed that the electrotonic architecture of these neurons scaled roughly in a MET-conserving mode. In conclusion, our results suggest only a minor impact of the Ras protein

* Corresponding author. Tel.: +49 341 9732234; fax: +49 341 9732299.
E-mail address: schierwa@informatik.uni-leipzig.de (A. Schierwagen).

0025-5564/$ - see front matter
doi:10.1016/j.mbs.2006.08.019

on dendritic electroanatomy, with non-significant changes of most regions of the corresponding METs.

Keywords: Pyramidal neurons; Dendritic morphology; Dendrogram; Scaling; Morphoelectrotonic transform

1. Introduction

Most neurons of the mammalian central nervous system exhibit a wide variety of branched dendritic trees. The recent advances in recording and staining techniques as well as in computer-assisted methods of acquiring digitized neuronal morphology in 3D have boosted attempts to reveal dendritic structure–function relationships [1].

According to the current view, dendritic morphology is seen as the structural correlate for receiving and processing inputs to a neuron. In evolution and development, the size of neurons with their dendrites has changed. An interesting question then is what the design principles and the functional consequences of enlarged or shrinked dendritic trees might be [2].

The adoption of transgenic mice mutants has provided a new means to investigate this problem, among others. Transgenic mice mutations serve for understanding gene function, as well as for developing therapies for genetic diseases. In these mutants, the gene overexpression may affect several organs and tissues, including the brain.

In a specific mouse mutant (introduced by [3] and referred to as synRas mice), a permanently active Ras protein (Val12-Ha-Ras) in post-mitotic neurons is expressed. In this mutant the expression of Ras starts post-natally around day 15, when neurons are post-mitotic and the majority of synaptic contacts has been established. The volume of the neocortex of synRas mice is expanded up to 25% as compared to wildtype mice. In particular cortical pyramidal neurons express the synRas construct at high levels resulting in a dramatically enlarged volume of the cortical pyramidal cells which is mainly caused by increased dendritic diameter and tree degree [4,5]. The number of neurons, however, remains unchanged [3].

Changes are generally more prominent in layer V than in layers II/III. Topological analyses [6] revealed significant differences between synRas and wildtype mice regarding any parameters considered, i.e., number of intersections, branching points (nodes) and tips (leaves), in both basal dendrites and the apical arbor of layer V neurons but not of layers II/III neurons. In subsequent studies these findings have been substantiated [7,8].

The significance of such changes in dendritic morphology to a neuron's capabilities for receiving and processing inputs could be examined in various ways. Using compartmental models of reconstructed cortical neurons and model neurons, recent simulation studies have investigated the role of branching complexity and spatial distribution of dendritic volume in determining neural integration, synaptic plasticity, and the firing patterns that define neuronal function [9–11].

In this study, we employed compartmental modeling to simulate the electrotonic properties of both wildtype and synRas pyramidal neurons. In particular, we used the morphoelectrotonic transform (MET, cf. [12,23]) to explore the scaling mode realized by the larger dendritic trees of synRas pyramidal cells.

2. Materials and methods

2.1. Experimental basis and reconstructions

We used data derived from experiments with three synRas mice aged nine months (see [3] for the establishment of the synRas mouse line), as well as with three wildtype mice of the same age. The details of experimental procedures have been described elsewhere [4].

The main deliverables were two sets of retrogradely labelled pyramidal cells (28 cells from wildtype and 26 cells from transgenic mice) which were reconstructed (Fig. 1) using Neurolucida™ (MicroBrightField, Inc.). The system allowed accurate tracing of the cell processes in all three dimensions and continuous adjustment of the dendritic diameter with a circular cursor. A motorized stage with position encoders enabled the navigation through the section in the *xyz* axes and the accurate acquisition of the spatial coordinates of the measured structure. All visible dendrites were traced without marking eventual truncation of smaller dendritic sections. This may have led to certain underestimation of the dendritic tree, especially in synRas mice with a larger dendritic arbour. To gain both optimal transparency for optimal tracing facilities and at the same time a possibly complete neuronal reconstruction, sections of 160 μm thickness were used. Thicker sections allowed only ambiguous tracing of thinner dendritic branches. Shrinkage correction (300%) was carried out in the Z axis, but not in the XY plane, because shrinkage was negligible in these dimensions ($\sim$10%).

2.2. Editing and conversion of morphology files

The morphology files created in this way were processed to allow further analyses. We used for this purpose the freely available program CVAPP [13], a cell viewing, editing and format converting program for morphology files (Fig. 1). It can be also used to prepare structures digitized with Neurolucida™ software for modeling with simulators like Neuron and Genesis.

In particular, CVAPP has been used to convert Neurolucida ASCII files to the SWC format describing the structure of a neuron in the simplest possible way [14]. In this format, each line

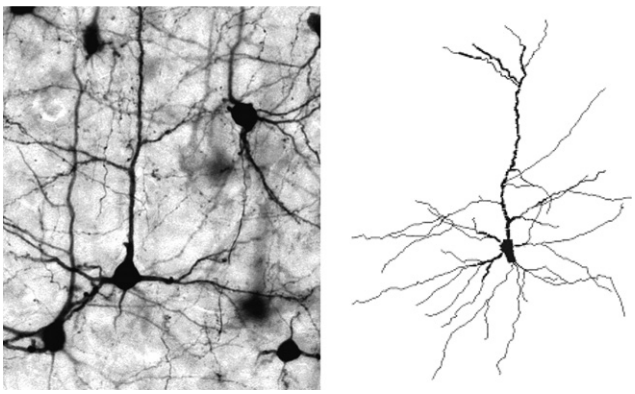

Fig. 1. Light micrograph of retrogradely labelled pyramidal neurons from layers II/III of the synRas mouse neocortex (left) and a pyramidal cell (right) rendered with CVAPP.

encodes the properties of a single neuronal compartment. The format of a line in an SWC file is as folllows: *nTxyzRP*. In turn, these numbers mean: (1) an integer label (normally increasing by one from one line to the next) that identifies the compartment, (2) an integer that represents the type of neuronal segment (0—undefined, 1—soma, 2—axon, 3—dendrite, 4—apical dendrite, etc.); (3–5) *xyz* coordinate of compartment, (6) radius of compartment, (7) parent compartment (defined as −1 for the initial compartment).

2.3. Terminology for dendrites

The dendrites of a neuron are modeled as trees of segments emanating from the soma. A segment is defined as a portion of dendrite extending between two branching points (intermediate segments), or between a node (branching point) and a tip (terminal segments). Dendritic segments are approximated by cylindric sections of length l and diameter d.

The distance from the soma to a point on the dendritic tree measured along the course of the segments lying inbetween is the path length which is generally greater than the Euclidean distance between the corresponding points.

Dendritic trees may be categorized by topological type depending on the patterning of segments, independently of metrical and orientation features [15].

Parameters mostly used are *order* and *degree* (Fig. 2). The *order* (γ) represents the topological distance from the soma. Its value is an integer incremented at every bifurcation ('centrifugal order'). A value of $\gamma = 0$ is assigned to the primary segments, i.e., those emerging directly from the soma. The *degree* (n) represents the number of tips of a subtree (or partition) stemming from a segment. In a binary tree, it is related to m, the number of segments of the partition, by $m = 2n - 1$.

The dendritic systems of pyramidal cells are divided into basal and apical parts. Each of the subdivisions is considered separately (see Section 3).

2.4. Theoretical basis

The potential spread along any of the branches is governed by the one-dimensional cable equation [16,17]

$$\tau_m \frac{\partial V(x,t)}{\partial t} = \lambda^2 \frac{\partial^2 V(x,t)}{\partial x^2} - V(x,t) - R_{\text{in}} \cdot I(x_0,t), \tag{1}$$

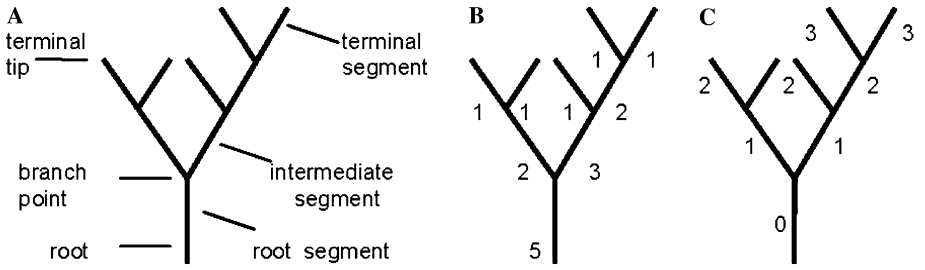

Fig. 2. Topological representation of a dendrite. (A) The tree is depicted by a set of connected segments which are labeled by (B) the degree of their subtrees and (C) their centrifugal order.

where $V(x,t)$ is the membrane potential at time t and position x, $\tau_m = R_m C_m$ is the membrane time constant, $\lambda = \sqrt{dR_m/(4R_i)}$ is the length constant, and $I(x_0,t)$ is the current injected at point x_0 where the input resistance is R_{in}. The electrical membrane parameters C_m, R_m and R_i are the membrane capacitance, resistance and axial resistivity, respectively.

The electrotonic distance X is defined then as $X = x/\lambda$, i.e., physical distance x normalized by λ. Therefore, the electrotonic length of a finite cable segment of length l is $L = l/\lambda$. A generalized expression for dimensionless distance between two points a and b is [18] $X = \int_a^b \frac{dx}{\lambda(x)}$ which has been used to derive analytical solutions to cables of varying cross-sectional area or membrane properties [19,20].

In an infinite cylindric cable the steady-state solution to Eq. (1) is

$$V(x) = V(0) \cdot \exp\left(-\frac{x}{\lambda}\right) \tag{2}$$

with current injection site at $x = 0$. Obviously, in this case the natural logarithm of the voltage attenuation $V(x)/V(0)$ gives the electrotonic distance

$$X = \ln \frac{V(x)}{V(0)} = \frac{x}{\lambda}. \tag{3}$$

2.5. Compartmental modeling and morphoelectrotonic transform

Compartmental models represent a neuron as an equivalent electrical circuit composed of isopotential compartments with each having a resistance and capacitance to ground and are linked together by ohmic resistances (Fig. 3).

From the mathematical point of view, the parabolic partial differential Eq. (1) is approximated by a set of ordinary differential equations which must be solved numerically [21].

Simulations with the compartment models were done with the NEURON simulator [22] on a PC under Windows XP. Membrane properties were uniform throughout the model cells. We used

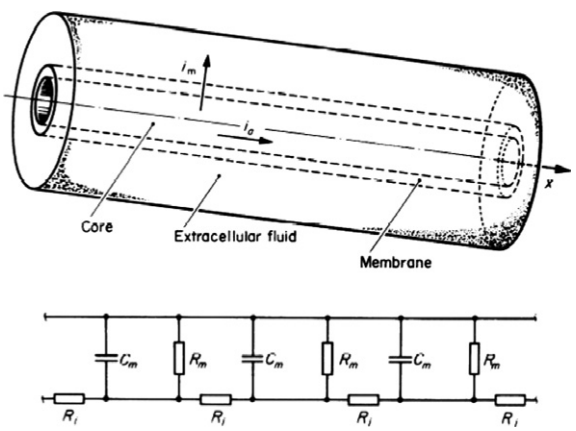

Fig. 3. Scheme of a membrane cylinder and its equivalent electrical circuit. For details, see text.

typical estimates of the biophysical properties: $R_i = 150\ \Omega\,\mathrm{cm}$, $R_m = 70\ \mathrm{k}\Omega\,\mathrm{cm}^2$, and $C_m = 1\ \mu\mathrm{F}/\mathrm{cm}^2$.

The simulations were used to compute the morphoelectrotonic transform (MET) of each neuron. The MET maps the neuron from anatomical space into electrotonic space, using the logarithm of voltage attenuation as the distance metric. This transformation was described by several authors [12,23]. In the following, the approach of these authors is outlined.

The key to this transformation is the new definition of electrotonic distance L_{ij} between two locations i, j on a neuron as given in (3), i.e., through the natural logarithm of the voltage (or current) attenuation. If voltage V_i is applied at point i, the response V_j at point j is obtained, and the voltage attenuation from i to j is

$$A_{ij} = \frac{V_i}{V_j}. \tag{4}$$

Vice versa, voltage V_j applied at point j leads to the response V_i at point i, and the voltage attenuation from j to i is

$$A_{ji} = \frac{V_j}{V_i}. \tag{5}$$

It was shown [24–26] that in general the two attenuations are not equal to each other, $A_{ji} \neq \mathrm{A}_{ij}$, i.e., signal attenuation between any two points in a real cell is direction-dependent.

Electrotonic distance from site i to j is defined as

$$L_{ij} = \ln A_{ij}. \tag{6}$$

In the case of an infinite cylinder, L_{ij} equals the classical measure X defined in (3) where voltage decays e-fold per unit of distance for both metrics. As we see from (6), L_{ij} preserves this property of e-fold decay for networks of finite cables such as dendritic trees. This is not true for the classical measure X (see [12,23]).

If stimulus and recording location are interchanged, the electrotonic distance is $L_{ji} = \ln A_{ji}$. Therefore, the path in anatomical space between any two points on the neuron has two mappings in electrotonic space, depending on direction of signal spread.

From the definition (6) of electrotonic distance the additivity property of this measure follows, as we easily see from the following. If point k lies somewhere on the direct path between points i and j, then $A_{ij} = A_{ik} \cdot A_{kj}$, and (6) yields $L_{ij} = L_{ik} + L_{kj}$.

The properties of the log-attenuation measure allow a clear and instructive visual representation of electrotonic architecture. Generating the morphoelectrotonic transform (MET) of a neuron from its morphological and electrical properties requires a two-step procedure. First, the log-attenuations for a set of points relative to some reference site (e.g., the soma) are calculated. This is done for several frequencies, because both steady-state and dynamic signals are considered. Since attenuation is direction-dependent, a pair of transforms must be computed for each dendritic segment. Usually the soma is taken as one fixed reference point, and somatopetal (V_{in}) and somatofugal (V_{out}) mappings are computed. Second, graphical representations are constructed—METs—in which the anatomical length of each of the segments comprising the dendritic tree is replaced by its corresponding L_{ij}. Diameter and orientation of the segment are preserved.

The neural simulation environment NEURON [22] includes electrotonic analysis tools enabling the MET calculation in a convenient way. We calculated METs at two different frequencies (0 and 50 Hz) and for somatopetal and somatofugal inputs, i.e., four METs per neuron.

2.6. Data analysis and statistics compiled

In this paper, we performed scaling measurements on dendrogram representations [27] of neurons in metric MET space where the distance metric is defined through the log-attenuation of membrane potential (see Section 2.5). In a dendrogram representation, dendritic segments are straightened out and oriented parallel to the primary axis of the stem segment. Distances measured along this axis correspond to path lengths on the dendrite (Fig. 4).

The scaling properties of pyramidal neuron dendrites were analyzed by using exclusively the MET dendrogram data. In electrotonic transform space, we performed two different measures of dendritic complexity. First, a variant of Sholl analysis [6] was performed, i.e., dendrograms were quantified. Probe lines are laid across the dendrogram at regular intervals and the number of dendritic intersections with each line is plotted as a function of dendritic path length from the soma.

We also performed an order analysis of electrotonic lengths, i.e., the number of segments was calculated as a function of segment order and the median of MET lengths at a given segment order was calculated.

Since the Kolmogorov–Smirnov test for normal distribution failed in general, we used the Mann–Whitney U test for independent groups. A series of between-class comparisons (wildtype vs. transgenic) was carried out for each measure of electrotonic extent, testing the null hypothesis that the two sample data stem from the same population, i.e., that the Ras protein has no effect on electrotonic architecture.

The significance level was set at $P < 0.05$ and computations were performed using the SPSS 12.0 statistical package. The photomicrograph (Fig. 1) was taken with a digital microscope camera AxioCam HRc running on AxioVision 3.1 software (both from Carl Zeiss Vision).

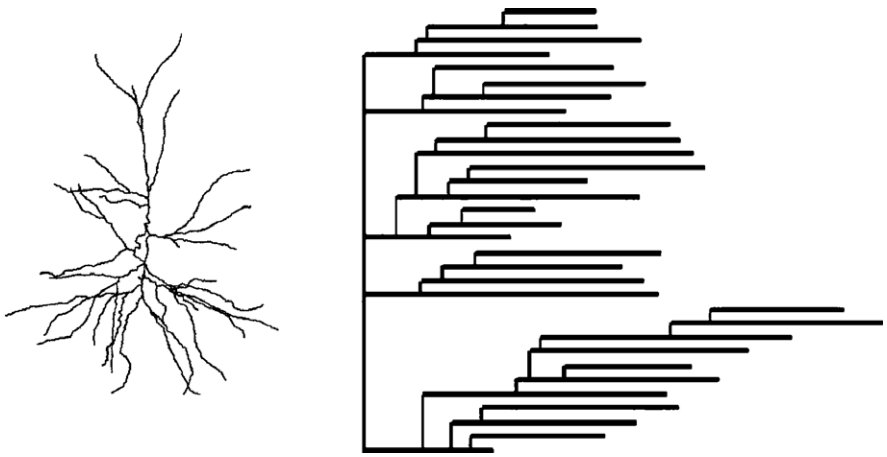

Fig. 4. A transgenic neuron (SE 19) as displayed in anatomical space (left) and dendrogram space (right).

3. Results

The morphology and electrotonic architecture of a representative neocortical pyramidal neuron from synRas mouse is shown in Fig. 5. On the left of this figure, the 2D projection of the anatomy of the cell is displayed. The center and right images are the renderings of the V_{in} and V_{out} morphoelectrotonic transforms relative to the soma at frequencies of 0 and 50 Hz. The calibration bars are in 'log attenuation' units (one unit of separation in electrotonic space corresponds to an e-fold decay of voltage). Because the soma is the reference point for the transforms shown in this and the following figure, electrotonic distance is to be measured *away* from the soma in the V_{out} image, and *toward* it in the V_{in} image.

It should be noticed that neurons are electrotonically more compact for somatofugal signal propagation (V_{out}) than for somatopetal propagation (V_{in}) which means that there is only slight attenuation of voltage spread away from soma. The proximal segments account for most of the voltage attenuation for somatofugal propagation, but the terminal branches are where most of the signal loss occurs during somatopetal propagation.

The basilar dendritic field is electrotonically more compact than the apical field for V_{out}, but for V_{in} these fields are nearly equally extensive (see also Fig. 6).

V_{out} transforms at 0 Hz of both neuron classes are relatively compact while they grew at 50 Hz, indicating in both cases moderate voltage attenuation away from soma. The V_{in} transforms were a multiple larger (note different scales in the V_{in} and V_{out} plots).

Sholl analyses of the wildtype and synRas samples yielded a differentiated picture for apical and basal dendrites depending on input frequency and direction of signal spread (Fig. 6). Apical dendrites of both samples showed no differences in their Sholl plots, neither for the two input frequencies used (0 and 50 Hz) nor for the V_{in} and V_{out} transforms (Fig. 6). Generally, the spatial extent of the dendritic trees in both V_{in} and V_{out} transforms increased roughly threefold from 0 to 50 Hz input frequency. For the two samples, the extent of the apical tree V_{out} transforms exceeds that of the basal dendrites by almost two while the V_{in} transforms nearly agree in extent.

In the V_{in} transform at DC input, the number of dendritic intersections with the probe lines reaches a maximum very near to soma, at distance (path length) $L = 0.1$, while at 50 Hz the maximum is shifted to distance $L = 1.2$.

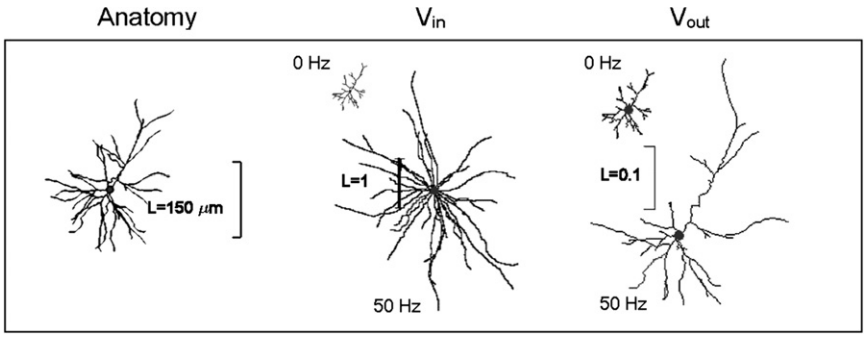

Fig. 5. Mapping from anatomic to electrotonic space. Left: 2D projection (scale bar: 150 μm) of the anatomy of a transgenic neuron (SE 19). Middle and right: renderings of each METs computed at 0 Hz (top) and 50 Hz (center) for somatopetal (V_{in}—scale bar: $L = 1$) and somatofugal (V_{out}—scale bar: $L = 1$) signal propagation.

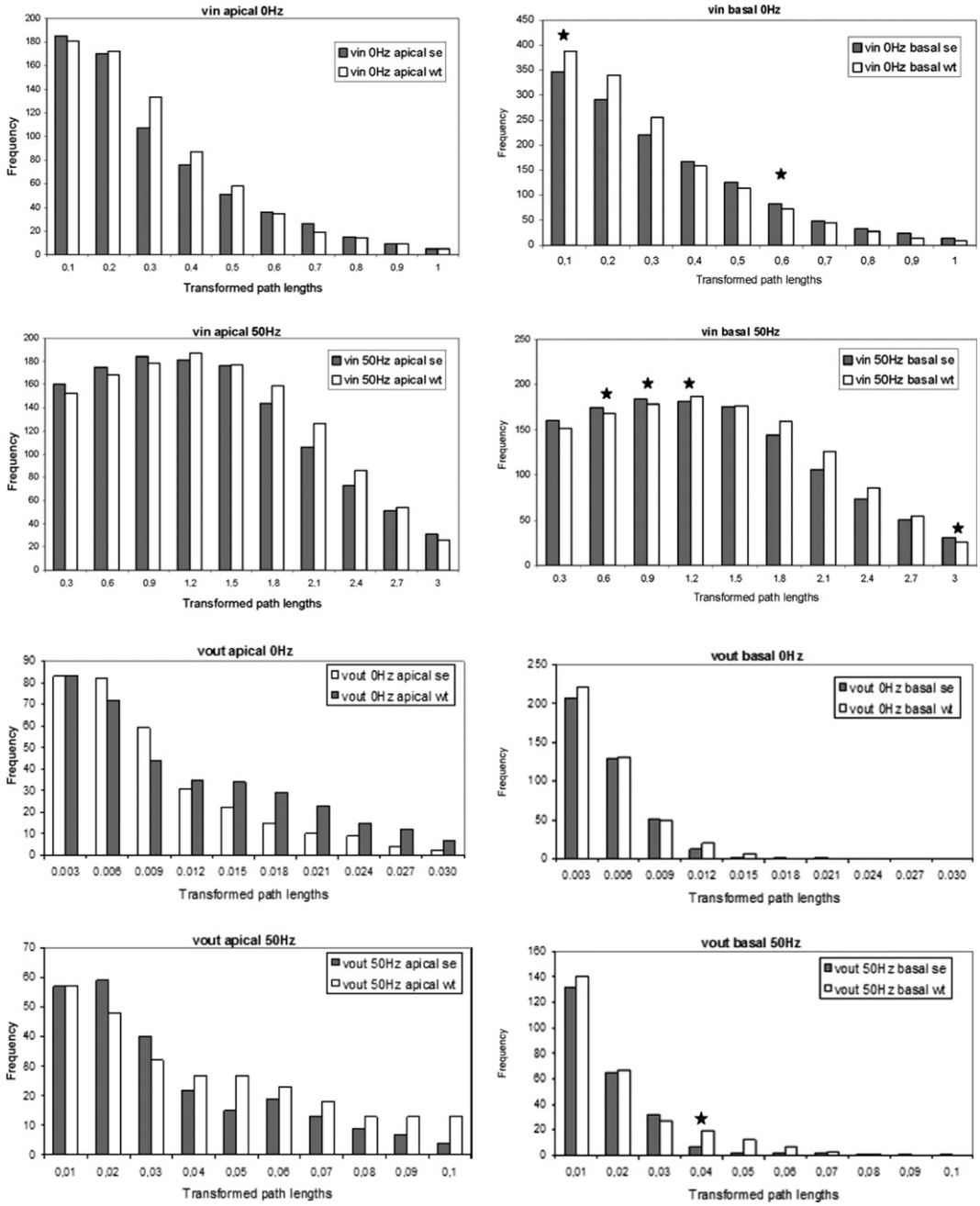

Fig. 6. Sholl analyses of MET dendrograms. Displayed is the frequency of dendritic intersections as a function of transformed path lengths from the soma in the V_{in} (upper part) and V_{out} (lower part) transform. Apical dendrites (left column) and basal dendrites (right column each) were analyzed for input frequencies of 0 Hz (upper row each) and 50 Hz (lower row each). Note the different scales of the distance variable for the two input frequencies in the V_{in} and V_{out} analyses, respectively. Asterisks (*) denote significant differences ($P < 0.05$) between the two groups. Abbreviations: wt, wildtype neurons; se, synRas neurons.

The V_{out} transforms at DC input have maximal number of dendritic intersections at distances in the region $L = 0.003$–0.006 and at 50 Hz the maximum lies at distance $L = 0.02$.

In the V_{in} transform at 50 Hz of basal dendrites, the number of dendritic intersections differs significantly at several distances ($L = 0.6$, 0.9, 1.2 and 3.0). In addition, at DC input differences appeared at $L = 0.1$ and 0.6. In the V_{out} transforms at 50 Hz only the numbers of dendritic intersections at $L = 0.04$ differ significantly. Note the different shapes of the Sholl plots for the V_{in} but not the V_{out} transforms at input frequencies of 0 and 50 Hz.

The order analysis of electrotonic lengths was performed following a centrifugal ordering scheme (Fig. 7). The number of dendritic segments per order was calculated (not shown) and MET lengths were displayed as sample medians per segment order. Interestingly, the results yielded a distinct picture if compared with the Sholl analyses of the METs. V_{out} transforms (but not V_{in} transforms) of apical dendrites showed clear differences at frequency 50 Hz for orders 2, 5 and 9 (the latter also at DC). In contrast, basal dendrites appeared unchanged (except V_{in} at 50 Hz, order 6). An additional order appears in the synRas neurons (order 8).

It appears as if in the V_{in} transform of basal dendrites at 50 Hz the significant increases in segment numbers at some distances ($L = 0.6$, 0.9, 1.2 and 3.0) are confined to order 6. On the other hand, the differences in the V_{out} transforms of apical dendrites at frequency 50 Hz for some orders (2, 5 and 9) had no counterpart in differences of Sholl diagrams.

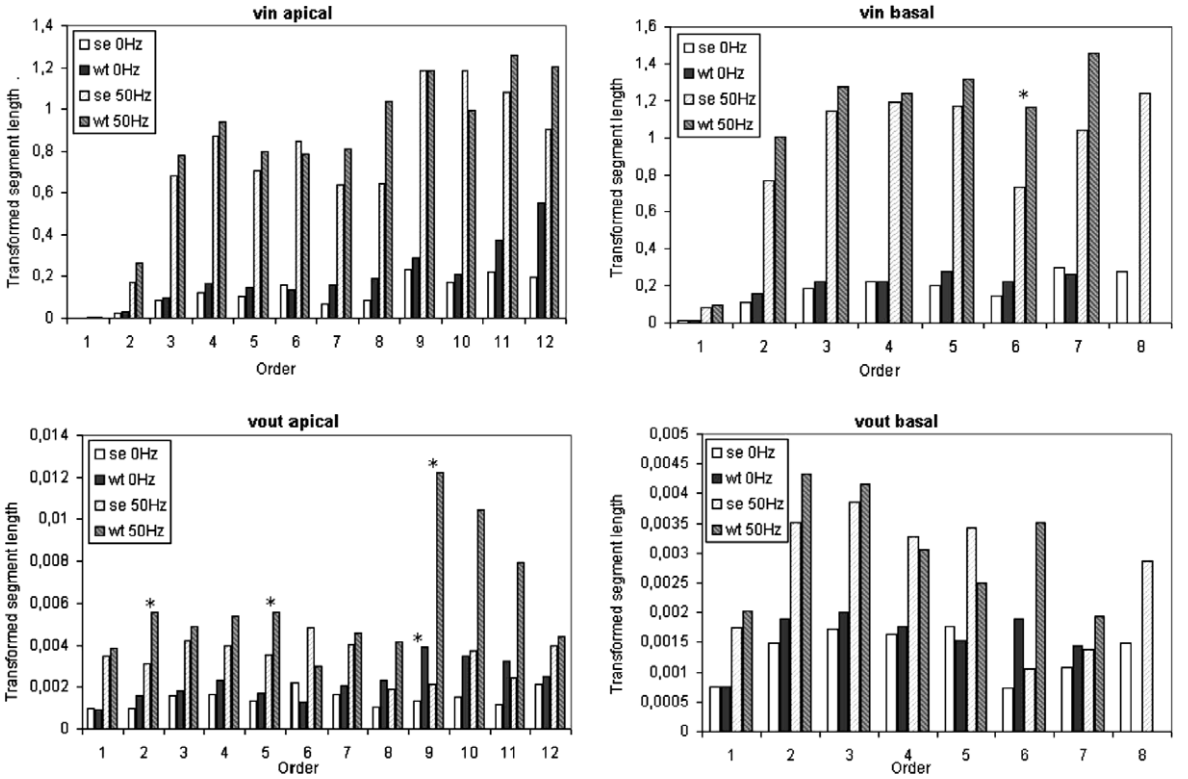

Fig. 7. Order analysis. MET segment lengths are displayed as sample medians depending on segment order. Significant differences ($P < 0.05$) between the two groups are denoted by *.

Together the Sholl and order analyses demonstrate that both basal and apical dendrites in synRas neurons underwent only a few localized changes in their MET properties at 50 Hz but not at DC.

4. Discussion

The traditional way to explore onto- and phylogenetic changes at various levels of brain organization has been by means of comparative anatomical analyses on normal and pathological brains. As yet, only a few studies have examined the effects of neuron size changes on function. Two theoretical scaling modes have previously been analyzed, conservative (isoelectrotonic) scaling, and isometric scaling [28]. They are only two among many tree patterns in which the diameters of dendritic segments change according to a functional relationship to their increase in length. From cable-theoretic analyses, it is known that conservative scaling preserves the passive and active response properties, and isometric scaling steps up low pass-filtering of inputs. It has been suggested that both scaling modes were verified in neuroanatomical studies (see [29] and the references therein). These studies have often been based, however, either on a few examples (small sample size), or on rough measures like maximal extent in anatomical and/or electrotonic space, but not on detailed analyses of dendritic architecture including complexity measures. Therefore, the conclusions should be considered with caution.

Thus, there has been a need to consider the scaling problem of neurons on the basis of large sample data. This study presented one of the rare quantitative analyses of large samples of neurons with respect to their electrotonic architecture (see [30] for another example). We used 3D data on neuronal morphology to quantitatively characterize the scaling properties of synRas neocortical neurons. Two sets of neurons, i.e., pyramidal cells from wildtype and synRas transgenic mice, have been analyzed.

In a previous study, a striking increase of dendritic tree size was verified in the pyramidal neurons of synRas mice neocortex [4]. Surface area and volume of proximal and intermediate dendritic segments were significantly augmented which was caused mainly by increased dendritic diameter, and not by segment elongation. No significant changes were seen in the number of dendritic segments; in some cases, however, additional orders were observed. Dendritic complexity as quantified by Sholl analyses of basal and apical dendrites was unaltered, too.

Given these different results from our morphometric analyses, differences between the morpho-electrotonic transforms of wildtype and transgenic neurons could be supposed. From cable and two-port theory the conclusion can be drawn, however, that the degree to which neuronal morphology is distorted by the MET is determined by a complicated interplay of segment diameter and boundary effects (see [12,23]). Predictions based solely on morphological measurements of how the METs of wildtype and transgenic neocortical pyramidal neurons may differ are therefore not possible.

Thus, the statistical analysis of the sample MET dendrograms computed with NEURON revealed features of their electroanatomy previously unknown. The results indicated a MET-conserving scaling mode. This means, the electrotonic architecture of these neurons scaled roughly in a way preserving both centrifugal and centripetal METs for the input frequencies applied. Dimensions of dendritic segments changed in such a way that direction- and frequency-dependent signal propagation in the passive neuron models was generally not affected.

In conclusion, our results suggest only a minor impact of the Ras protein on dendritic electroanatomy, with non-significant changes of most regions of the corresponding neuromorphic transforms. It remains an important problem for future research to examine how active membrane currents in the dendrites might influence the scaling properties of these neurons.

Acknowledgements

We thank our students A. Schubert, S. Jäger and E. Rose for technical contributions to the morphometric and electrotonic analyses. This work was supported in part by Deutsche Forschungsgemeinschaft (Grant GA 716/1-1).

References

[1] G. Stuart, N. Spruston, M. Häusser (Eds.), Dendrites, Oxford University Press, Oxford, 1999.
[2] J.M. Bekkers, C.F. Stevens, Two different ways evolution makes neurons larger, Prog. Brain Res. 83 (1970) 37.
[3] R. Heumann, Ch. Goemans, D. Bartsch, K. Lingenhöhl, P.C. Waldmeier, B. Hengerer, P.R. Allegrini, K. Schellander, E.F. Wagner, T. Arendt, R.H. Kamdem, K. Obst-Pernberg, F. Narz, P. Wahle, H. Berns, Constitutive activation of Ras in neurons promotes hypertrophy and protects from lesion-induced degeneration, J. Cell Biol. 151 (2000) 1537.
[4] A. Alpár, K. Palm, A. Schierwagen, T. Arendt, U. Gärtner, Expression of constitutively active p21H-ras^{Val12} in postmitotic pyramidal neurons results in increased dendritic size and complexity, J. Comp. Neurol. 467 (2003) 119.
[5] U. Gärtner, A. Alpár, G. Seeger, R. Heumann, T. Arendt, Enhanced Ras activity in pyramidal neurons induces cellular hypertrophy and changes in afferent and intrinsic connectivity in synRas mice, Int. J. Dev. Neurosci. 22 (2004) 165.
[6] D.A. Sholl, Dendritic organization in the neurons of the visual and motor cortices of the cat, J. Anat. (Lond.) 87 (1953) 387.
[7] L.F. Costa, M.S. Barbosa, A. Schierwagen, A. Alpár, U. Gärtner, T. Arendt, Active percolation analysis of pyramidal neurons of somatosensory cortex: a comparison of wildtype and p21H-ras^{Val12} transgenic mice, Int. J. Mod. Phys. C 16 (2005) 655.
[8] A. Schierwagen, L.F. Costa, A. Alpár, U. Gärtner, T. Arendt, Neuromorphological phenotyping in transgenic mice: a multiscale fractal analysis, Proceedings of the European Conference on Mathematical and Theoretical Biology (ECMTB 2005), Birkhäuser Boston, Basel (2007).
[9] Z.F. Mainen, T.J. Sejnowski, Influence of dendritic structure on firing pattern in model neocortical neurons, Nature 382 (1996) 363.
[10] J.L. Krichmar, S.J. Nasuto, R. Scorcioni, S.D. Washington, G.A. Ascoli, Effects of dendritic morphology on CA3 pyramidal cell electrophysiology: a simulation study, Brain Res. 941 (2002) 11.
[11] A. van Ooyen, J. Duijnhouwer, M.W. Remme, J. van Pelt, The effect of dendritic topology on firing patterns in model neurons, Network 13 (2002) 311.
[12] K.Y. Tsai, N.T. Carnevale, B.J. Claiborne, T.H. Brown, Efficient mapping from neuroanatomical to electrotonic space, Network 5 (1994) 21.
[13] R.C. Cannon, Structure editing and conversion with cvapp (2000). Available from: <http://www.compneuro.org/CDROM/nmorph/usage.html/>.
[14] D. Jaeger, Directions on how to use cvapp to convert Neurolucida v3 files to Genesis 2.1.p file format (2000). Available from: <http://www.compneuro.org/CDROM/docs/fileconversion.html>.
[15] J. van Pelt, A. Schierwagen, Morphological analysis and modeling of neuronal dendrites, Math. Biosci. 188 (2004) 147.

[16] J.J.B. Jack, D. Noble, R.W. Tsien, Electric Current Flow in Excitable Cells, second ed., Oxford University Press, Oxford, 1983.
[17] W. Rall, Cable theory for dendritic neurons, in: C. Koch, I. Segev (Eds.), Methods in Neuronal Modeling, MIT Press, Cambridge, MA, 1989, p. 9.
[18] W. Rall, Theory of physiological properties of dendrites, Ann. NY Acad. Sci. 96 (1962) 1071.
[19] A. Schierwagen, A non-uniform equivalent cable model of membrane voltage changes in a passive dendritic tree, J. Theor. Biol. 141 (1989) 159.
[20] M. Ohme, A. Schierwagen, An equivalent cable model for neuronal trees with active membrane, Biol. Cybernet. 78 (1998) 227.
[21] W. Rall, Theoretical significance of dendritic tree for input–output relation, in: R.F. Reiss (Ed.), Neural Theory and Modeling, Stanford University Press, Stanford, CA, 1964, p. 73.
[22] M.L. Hines, N.T. Carnevale, The NEURON simulation environment, Neural Computat. 9 (1997) 1179.
[23] A.M. Zador, H. Agmon-Snir, I. Segev, The morphoelectrotonic transform: a graphical approach to dendritic function, J. Neurosci. 15 (1995) 1669.
[24] E.G. Butz, J.D. Cowan, Transient potentials in neurons with arbitrary geometry, Biophys. J. 14 (1974) 1.
[25] N.T. Carnevale, D. Johnston, Electrophysiological characterization of remote chemical synapses, J. Neurophysiol. 47 (1982) 606.
[26] C. Koch, T. Poggio, V. Torre, Retinal ganglion cells: functional significance of dendritic morphology, Phil. Trans. R. Soc. 298 (1982) 227.
[27] P. Rothnie, D. Kabaso, P.R. Hof, B.I. Henry, S.L. Wearne, Functionally relevant measures of spatial complexity in neuronal dendritic arbors, J. Theor. Biol. 238 (2006) 505.
[28] O.H. Olsen, F. Nadim, A.A.V. Hill, D.H. Edwards, Uniform growth and neuronal integration, J. Neurophysiol. 76 (1996) 1850.
[29] R. Kötter, M. Feizelmeier, Species-dependence and relationship of morphological and physiological properties in nigral compacta neurons, Prog. Neurobiol. 54 (1998) 619.
[30] N.T. Carnevale, K.Y. Tsai, B.J. Claiborne, T.H. Brown, Comparative electrotonic analysis of three classes of rat hippocampal neurons, J. Neurophys. 78 (1997) 703.